Published in final edited form as:
J Phys Chem B. 2011 December 1; 115(47): 13935–13942. doi:10.1021/jp207607r.

NMR Studies of Localized Water and Protein Backbone Dynamics in Mechanically Strained Elastin

Cheng Sun, **Odingo Mitchell**, **Jiaxin Huang**, and **Gregory S. Boutis***
Department of Physics, Brooklyn College of The City University of New York, Brooklyn, New York 11210, United States

Abstract

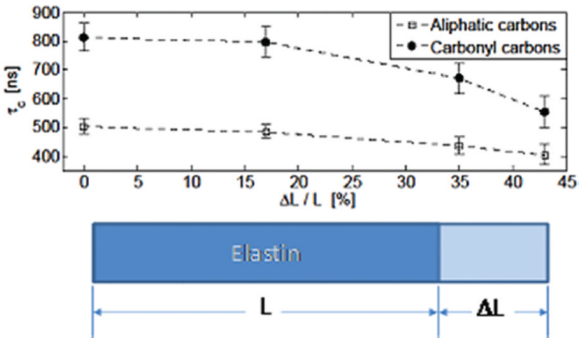

We report on measurements of the dynamics of localized waters of hydration and the protein backbone of elastin, a remarkable resilient protein found in vertebrate tissues, as a function of the applied external strain. Using deuterium 2D T_1–T_2 NMR, we separate four reservoirs in the elastin–water system characterized by water with distinguishable mobilities. The measured correlation times corresponding to random tumbling of water localized to the protein is observed to decrease with increasing strain and is interpreted as an increase in its orientational entropy. The NMR T_1 and $T_{1\rho}$ relaxation times of the carbonyl and aliphatic carbons of the protein backbone are measured and indicate a reduction in the correlation time as the elastomer strain is increased. It is argued, and supported by MD simulation of a short model elastin peptide $[VPGVG]_3$, that the observed changes in the backbone dynamics give rise to the development of an entropic elastomeric force that is responsible for elastins' remarkable elasticity.

INTRODUCTION

Elastin is an elastomeric protein that provides many vertebrate tissues with their remarkable resilient properties. The human aortic valve, for instance, is largely composed of elastin and undergoes several billion stretch strain cycles in the course of one's lifetime and typically only fails once – or more than once, if one is so lucky. Unlike other naturally occurring elastomers, such as the rubber of *Hevea brasiliensis* or highly elastic and tensile silk produced by the *Caerostris darwini*, elastin's function hinges on hydration.[1–4] The complex structure and hydration-dependent functional properties of this system have been of long-standing interest since Partridge's original work in isolating elastin from other tissue constituents.[5] In an effort to understand the source of elasticity, various models have been proposed based on thermodynamic methods[6] or studies that aimed at probing the complex

***Corresponding Author** gboutis@brooklyn.cuny.edu.

microscopic structure of the protein.[7–10] At present, a largely accepted notion is that the mechanism for elasticity is entropic in nature. In this, and all other models of elasticity, hydrating localized water is tacitly assumed, yet its contribution to the entropic mechanism of elasticity has eluded experimentalists. This work reports on a direct measurement of the correlation times of the localized waters of hydration as a function of the applied strain to the biopolymer, and provides further insight into the nature of the elastomeric entropic force borne by the protein backbone.

An important and intriguing property of elastin is that it undergoes an inverse temperature transition—a process by which the protein expels water, develops a complex network of hydrogen bonds across the protein backbone, and shrinks with increasing temperature from approximately 10 to 37 °C.[1] This observation, coupled with the fact that elastin is not soluble in water or does not crystallize, has spurred several efforts that aimed at studying short, repeating peptide segments that mimic the inverse temperature transition of the protein.[1,2,11,12] A model was proposed, developed through several studies of the mimetic $(VPGVG)_n$ peptide, that incorporates suspended segments between β-turns.[13] In this model, termed the librational entropy mechanism (LEM), the suspended segments undergo large-amplitude low-frequency torsional oscillations. It is argued in the model that librational amplitudes are damped upon extension, giving rise to a decrease in the entropy of a given segment with increasing strain, providing the driving mechanism for elasticity.[13] The experimental findings of our work support the notion of entropic changes in the LEM model and provide further insight into the source of elasticity—specifically that the frequencies of the protein backbone motion increase with increasing strain and thus reduce its entropy upon extension.

MATERIALS AND METHODS

Nuclear magnetic resonance (NMR) experiments were performed on purified bovine nuchal ligament elastin purchased from Elastin Products Co., LLC. The samples studied were purified by the neutral extraction method of Partridge[5] and were suspended in a mixture of D_2O and H_2O with a volume ratio of 50:50 with 0.0003 g/mL of sodium azide added as a biocide. The elastin samples were then mechanically strained in 1.5 cm long, 5mm diameter glass tubes with both ends held by poly(tetrafluoro-ethylene) tape and sealed using ethylene–vinyl acetate. Four samples were prepared; the strains ($\Delta L/L$) on the samples were 0, 17, 35, and 43%, and are denoted I, II, III, and IV, respectively, in this work. After the experiments were performed on sample IV, the sample was released and measured after 72 h and is denoted sample V. The loss of water in any of the samples was less than 1% over the entire course of experiments. All the experiments were carried out on a 200 MHz Tecmag Apollo NMR spectrometer using a Doty solids NMR probe at 25 °C and regulated to within 1 °C. The NMR pulse sequence for 2D T_1–T_2 correlation experiments is illustrated in Figure 1.[14] In the 2D T_1–T_2 correlation experiments, $\tau = 0.3$ ms and a free induction decay (FID) of 2.4 s was acquired so that a T_2 relaxation time in the range of 1 ms to 1 s was measured. The delay t_1, shown in Figure 1, was incremented from 1 ms to 10 s to enable an accurate measurement of T_1 values from 10 ms to 1 s. The ^{2}H π/2 pulse time was 19 μs. In the ^{13}C experiments, the π/2 pulse time for ^{13}C was 9 μs. A radio frequency field strength of ω_e = 27.7 kHz was applied with ^{1}H SPINAL-64 decoupling during signal acquisition[15] and a phase cycling scheme was implemented in the cross-polarization (CP) experiment so that the resulting signal observed on the ^{13}C spectra results only from cross-polarized magnetization.[16]

Molecular dynamics (MD) simulations were performed at 25 °C using the OPLS-AA/L force field model[17] and a Berendsen thermostat[18] in GROMACS.[19] The peptide was terminated by ($-NH_2$) and (−COOH) groups at its N- and C-terminus, respectively. The

initial structure of the $[VPGVG]_3$ peptide simulated was a linear chain. The model system was placed in a 125 nm^3 cubic box solvated with 4074 water molecules using the SPC216 water model.[20] An energy minimization was performed using the method of steepest descent with the maximum step size set to 1 and the force tolerance set to 2000 kJ/(mol nm) to remove overlapping atoms.[21] Following the energy minimization step, we performed a short simulation restraining the peptide position and equilibrating the pressure for 10 ps before executing the full simulations. Two scenarios were studied: (a) without an applied pull force and (b) with the Gly13 atoms being fixed and a pull force being applied on the atoms of Val4 with a constant force equal to 50 000 kJ/mol nm. The simulation without an applied pull force was performed for 4 ns. Equilibration of the peptide structure was determined by monitoring the average root-mean-square displacement (rmsd) of the C_α positions of the entire peptide. Figure 2 highlights the rmsd averaged over all C_α atoms as a function of time. The figure demonstrates that after approximately 2 ns of simulation time the structure is equilibrated. The time scale required for equilibration of this short 15-residue elastin peptide is similar to that observed by others.[11] In the pull simulation, the starting structure was the determined equilibrated structure after 3 ns of simulation. Another 4 ns of simulation was performed with the 50 000 kJ/mol nm force applied. MD derived properties of the unstrained and strained $[VPGVG]_3$ peptide were determined over the last 1 ns of the 4 ns simulations.

RESULTS AND DISCUSSION

To study the dynamical properties of water in elastin, we employed the 2D T_1–T_2 nuclear magnetic resonance (NMR) technique (illustrated in Figure 1),[14] and measured the ^2H T_1 and T_2 relaxation times of water in deuterium hydrated elastin. In this 2D experiment, the T_2 relaxation times of a system are measured as a function of separate inversion recovery experiments that probe the T_1 relaxation times. As described in ref 14, applying a 2D inverse Laplace transform (ILT) of the experimental data, the T_1 and T_2 NMR relaxation times are correlated and are manifested into a peak in the 2D map. This relatively new experimental scheme has been applied with great success in studies of the dynamics of water in a variety of complex porous systems.[22–24] Sample raw data from the 2D experiment for three different values of t_1 is shown in Figure 3, of sample I. The resulting 2D ILT map is shown in Figure 4 as an example. Four peaks are observed in the figure, corresponding to four reservoirs of water with distinguishable dynamical properties; the 2D ILT maps for all samples studied showed only four components.

For a spin $I = 1$ nucleus, such as ^2H, the NMR relaxation times are governed to a good approximation by the nuclear quadru-polar interaction[25] and the T_1 and T_2 are given by

$$\frac{1}{T_1} = \frac{3}{40}\left(1+\frac{\eta^2}{3}\right) C_q\{J(\omega_D)+4J(2\omega_D)\} \quad (1)$$

$$\frac{1}{T_2} = \frac{1}{80}\left(1+\frac{\eta^2}{3}\right) C_q\{9J(0)+15J(\omega_D)+6J(2\omega_D)\} \quad (2)$$

where ω_D is the ^2H Larmor frequency, $C^q = \{[(eQ)/\hbar][\partial^2 V/\partial z^2]\}^2$ and η is the asymmetry parameter of the potential V. The spectral density is given by $J(\omega) = \tau_c/[1 + (\omega\tau_c)^2]$ with τ_c defined as the correlation time of the interaction of the nuclear quadrupolar moment with the surrounding electric field gradient of the ^2H nucleus.[25] For the case of the ^2H nuclei of a water molecule, this interaction is intramolecular in origin. Thus, the measured correlation time of the ^2H nucleus is a measure of the random tumbling of the individual water molecule.

Using eqs 1 and 2 and our measured values of T_1 and T_2, the τ_c of the various signals in the 2D ILT map were determined. Table 1 details the measured relaxation times and correlation times as a function of the strain on the elastomer. Component α_1 is free water, by virtue of the fact that $T_1 \approx T_2$. Using a T_2–T_2 exchange experiment, in a previously published work we verified that α_2 is water that resides between the elastin fibers and β is a mobile component that resides within the elastin fiber.[24] The water corresponding to the peak with the shortest T_1 and T_2 relaxation times, labeled γ in Figure 4, has been determined to be in closest proximity to the protein, also by the T_2–T_2 exchange experiment and by considering the correlation times of the least mobile components in the 2D ILT map. To be clear τ_c^{β}=53.1 ns and τ_c^{γ}=112 ns (for the data shown in Figure 1) and hence the component of water denoted γ represents water that is more restricted than that denoted β. One is reminded that free water has a correlation time of approximately 5 ps, and therefore components β and γ appear to both undergo restricted dynamics with the β component being more mobile. In this work, we study the changes in the correlation times of components β and γ as a function of mechanical strain. For samples I, II, III, and IV the correlation times are plotted in Figure 5a as a function of the strain applied to the elastomer. It is evident from the figure that the correlation times of both the highly localized waters of hydration, component γ, and the more mobile component β, decrease with increasing strain on the biopolymer.

As the measured ^{2}H correlation times for the ^{2}H nucleus in water are intramolecular in origin, a reduction in correlation time would correspond to increased tumbling motion of the water molecule. Therefore, Figure 5a indicates an increase in random tumbling of localized waters of hydration with increasing strain on the biopolymer. An increase in random tumbling would correspond to an increase in the available configurational space to any given water molecule and may therefore be interpreted as an increase in its orientational entropy. This experimental observation appears to rule out the prediction derived from previous short-time molecular dynamics simulations that suggested that the orientational entropy of waters hydrating hydrophobic groups decreases during pulling of the elastin mimetic peptide $(VPGVG)_{18}$.[26] The measured correlation times of localized waters of hydration in sample V (the sample that was strained by 43%) are tabulated in Table 1. The τ_c^{β} and τ_c^{γ} for sample V are within the error bars of sample I, indicating that the dynamics of the water in close proximity to the protein returned to what was observed in an unstrained sample when the applied strain was removed.

To study the dynamics of the protein backbone, we investigated the natural abundance ^{13}C NMR relaxation times. Direct polarization (DP) and ^{1}H → ^{13}C cross-polarization NMR experiments were performed,[16] and exemplary spectra are shown in Figure 6 from sample I. A pulse phase cycling scheme was implemented in the CP experiment such that the resulting signal observed on the ^{13}C spectra results only from cross-polarized magnetization. Two features are evident in the spectra. First, it is clear from the DP spectrum, shown in Figure 6a, that the signal for the carbonyl carbons (centered at 173 ppm) is clearly distinguishable from that of the aliphatic carbons (16–60 ppm) even without any magic angle spinning;[27] this allows us to distinguish these two signals and measure the respective relaxation times unambiguously. Second, the overall signal in the CP spectrum (Figure 6b) is smaller than that of the DP spectrum(Figure 6a), indicating a high degree of mobility for this system (a factor of 3.977 in gain is expected for cross polarization for the case of a rigid solid[16]). Similar spectral resolution was achieved on all samples studied.

Using the DP technique, we obtained the T_1 and $T_{1\rho}$ times for the carbonyl and aliphatic carbons of mechanically strained elastin. We point out that the measured ^{13}C T_1 times of the carbonyl and aliphatic carbons observed in our experiments for the unstrained sample are in good agreement with that measured in hydrated elastin performed at a field of 400 MHz.[27]

Given the low spectral resolution of the static sample, one cannot distinguish different signals in the aliphatic region and the dynamics of individual constituents may vary. However, the ^{13}C T_1 and ^{1}H $T_{1\rho}$ relaxation times measured on hydrated elastin using magic angle spinning methods at a similar temperature appeared to be similar for all aliphatic carbons.[27] In an experimental study of the dynamics of the elastin mimetic $[VPGVG]_3$, the ^{13}C $T_{1\rho}$ times for all aliphatic carbons also appear to be similar.[28] It is therefore reasonable to study the region by employing an effective T_1 and $T_{1\rho}$ relaxation time. In hydrated elastin, it has been demonstrated that the carbonyl chemical shift anisotropy is averaged to a great extent due to the high mobility of the hydrated protein.[27] The ^{13}C relaxation times are thus largely mediated by the nuclear carbon–proton dipolar interactions, and the T_1 and $T_{1\rho}$ are given by

$$\frac{1}{T_1}=\frac{1}{10}C_D\{J(\omega_H-\omega_C)+3J(\omega_C)+6J(\omega_H-\omega_C)\} \quad (3)$$

$$\frac{1}{T_{1\rho}}=\frac{1}{20}C_D\{4J(\omega_e)+J(\omega_H-\omega_C)+3J(\omega_C)+6J(\omega_H)+6J(\omega_H+\omega_C)\} \quad (4)$$

where ω_H and ω_C are the ^{1}H and ^{13}C Larmor frequencies respectively, ω_e is the spin-lock radio frequency field strength and $C_D=[(\hbar^2\gamma_C\gamma_H)/(r^3_{C-H})]^2$.[29] In the spectral density $J(\omega)$ in eqs 3 and 4, τ_c is the correlation time of the fluctuating dipolar field experienced by the ^{13}C spins.

It is important that one distinguishes the correlation time that appears in eqs 1 and 2 from that in eqs 3 and 4. The correlation time appearing in eqs 3 and 4 is related to fluctuations of the ^{13}C–^{1}H dipolar interaction. However, the correlation time in eqs 1 and 2 is related to fluctuations of the interaction of the ^{2}H nuclear quadrupole moment with the local electric field gradient.[25] For the case of the ^{2}H nuclei of water molecule, this interaction is intramolecular in origin and the correlation time of the ^{2}H nucleus is a measure of the random tumbling of the individual water molecule. However, the correlation time of the ^{13}C nucleus is governed by the overall relative motion of all ^{1}H–^{13}C internuclear vectors and accounts for vibration, translation and rotational motions. Lastly, we point out that we have modeled the fluctuation of the ^{13}C–^{1}H dipole–dipole field by a single spectral density in eqs 3 and 4, and that the derived correlation times from these expressions represent the average correlation time over all interactions.

Using eqs 3 and 4, and the measured ^{13}C T^1 and $T_{1\rho}$ relaxation times, the τ_c is determined for the carbonyl carbons and aliphatic carbons in all the samples. The measured relaxation times and correlation times are provided in Table 2, as a function of the applied strain on the elastomer. In addition, example relaxation data for the carbonyl carbon T_1 and $T_{1\rho}$ are provided in Figures 7 and 8, respectively. For the unstrained sample (sample I), referring to Table 2, we measured a correlation time of $(8.14 \pm 0.48) \times 10^{-7}$ s for the carbonyl carbons. Previous experimental studies of water hydrated calf ligamentum nuchae revealed that 80% of the carbonyl carbons undergo rapid segmental motion characterized by an average rotational correlation time of approximately 40 ns.[30] The method implemented to determine this correlation time involved a measurement of only a single relaxation time and the assumption of a simple model of elastin segmental motion. Nevertheless, the value in the unstrained sample measured in our work appears to be in close agreement with this value. In addition referring to Table 2, the measured overall aliphatic carbon correlation times measured in our work is $(5.04\pm0.28)\times10^{-7}$ s, and this value appears to be in close agreement with that measured in a short elastin mimetic peptide $[VPGVG]_3$ hydrated at 30% (an average value of approximately 1.6 μs is reported).[28] Our measured correlation times for the

aliphatic and carbonyl carbons are presented in Figure 5b as a function of the strain on the biopolymer. It is clear from the figure that the correlation times for both carbonyl and the overall aliphatic carbons decrease with increasing strain. The physics of this result dictates an increase in the fluctuation of the total carbon–proton dipolar field surrounding both carbonyl and aliphatic sites with increasing strain. Amazingly, the measured correlation times of the carbonyl and overall aliphatic carbons of sample V (the sample that was released after being strained 43%), tabulated in the Table 2, were within the experimental uncertainties of that observed in sample I illustrating the remarkable elastomeric properties of elastin!

To qualitatively describe the underlying physics of the experimental results shown in Figure 5b and the associated entropy changes, we have studied the model elastin mimetic peptide $(VPGVG)_3$ under mechanical strain by MD simulation. It should be noted, however, that a short time scale simulation of a short peptide may overlook certain properties associated with slow motions that can only be realized in experiments of the much larger, densely packed and highly cross-linked protein. To be clear, the purpose of the simulation is to shed some light on the physics of this complex system by studying a short model peptide—the model and simulation are not intended to capture all the dynamics of the elastin/water system. The rationale in choosing this peptide as a model system of elastin is as follows. Several experimental studies of elastin and short mimetic peptides consisting of repeats of $[VPGVG]_n$, including light scattering, circular dichroism, and nuclear magnetic resonance, have provided evidence of an inverse temperature transition.[1] More recently, molecular simulations performed on an elastin mimetic peptide $[VPGVG]_{18}$ have shown signatures of the inverse temperature transition of this peptide in the temperature range of 15–42 °C, and more details into its thermal behavior.[11] Molecular dynamics simulations have also suggested that a minimum threshold of proline and glycine residues may be responsible for providing elastin with a critical level of disorder required for elasticity.[31] Furthermore, the commonly repeating motifs found in human aortic elastin have been recently analyzed and it was determined that one of the topmost abundant 5-mer repeats is VPGVG, making it an important structural element of elastin.[32]

Various MD simulation derived properties of $[VPGVG]_3$ were determined over a time duration of 1 ns under relaxed and strained conditions and are tabulated in Table 3. Details relating to the simulation are provided in the Materials and Methods section. Table 3 highlights the radius of gyration and the root-mean-square fluctuation (rmsf) as determined by the position of the C_α, and the lifetime of peptide–water hydrogen bonds, as well as the increase in the number of water molecules within 0.6 nm of the peptide. For both the strained and relaxed states of the peptide the eigenvalues, λ_{ii}, of the mass-weighted covariance matrix of all atoms of the MD trajectory were computed. In computing the covariance matrix in the unstrained study, we used data ranging from the last 1 ns of the simulation where the structure was observed to equilibrate, as discussed in Materials and Methods. In the strain study, we used a total time frame of 1 ns to measure the covariance matrix. A quasi-harmonic approximation was applied whereby the frequencies, ω_i, of uncorrelated simple harmonic oscillators are given by $\omega_i = [(k_B T)/\lambda_{ii}]^{1/2}$.[33] The entropy of a harmonic oscillator with frequency ω_i at a temperature T is

$$S_i = k_B \left[\frac{\hbar\omega_i/k_B T}{e^{\hbar\omega_i/k_B T} - 1} - \ln(1 - e^{-\hbar\omega_i/k_B T}) \right] \quad (5)$$

An important result derived from the above expression is that the entropy of each mode, S_i, reduces as a function of frequency ω_i (see Figure 5 in ref 13). Figure 9 highlights the dependence of entropy as a function of frequency. The histograms of the frequencies derived from the simulations are plotted in Figure 10 for both scenarios studied. The resulting total

entropy of the peptide was determined by summing the entropy contribution of each frequency and is tabulated in Table 3. Figure 10 shows a shift in population to higher frequency when the peptide is strained. By analogy, one is reminded from solid-state physics that an applied strain to a solid induces a shift in vibrational frequency of the lattice.[34–38] According to eq 5, high frequencies contribute less to entropy, and thus Figure 10 implies a decrease in the total peptide entropy when strained; this is observed in the first row of our results tabulated in Table 3; the peptide reduces its entropy from 1.63 to 1.46 kJ/(mol K) upon being elongated. It should be noted that the entropy obtained by the quasi-harmonic approach can be overestimated in certain cases. As discussed in ref 28, eq 5 would approximate the entropy when fluctuations derived from a classical simulation are implemented, rather than fluctuations determined by a quantum mechanical simulation. If classical fluctuations are implemented, eq 5 is justified in the limit when $\omega \ll k_B T/\hbar$. In our toy-model simulation, $k_B T/\hbar$ is approximately 6.2 THz and a large fraction of the frequency components shown in Figure 10 satisfy this approximation. Although eq 5 breaks down in the limit of high-frequency quantum oscillations, they contribute less to the entropy compared to low-frequency components.

In the LEM model,[13] the peptide is treated as a series of quasi-harmonic oscillators undergoing low-frequency, large-torsional oscillations when relaxed; it is argued in the LEM model that the amplitude of the motion is reduced upon extension. The observed reduction of the amplitude of the backbone motion resulting from the strain, as quantified by the root mean square fluctuation (rmsf) of the C^{α} shown in Table 3, is consistent with the expected change according to the LEM model. Furthermore, the observation that higher frequency components are populated upon extension demonstrates that the frequency of the peptide oscillation increases when strained and thus reduces the peptide entropy.

Our experimental data, highlighted in Figure 5b, indicates that there is a decrease in the correlation times of both carbonyl and aliphatic carbons, implying that the motion of the carbon–proton fluctuating dipolar field of both regions increases with increasing strain. On the basis of the simulation results of the model elastin peptide discussed above, we attribute the decrease in the measured correlation times to an increase in frequency of the protein backbone motion. According to eq 5, the experimental results in Figure 5b imply a decrease in the entropy of the protein backbone as the strain is increased. Moreover, referring to Figure 5a, the measured decrease in correlation times of water indicates an increase in tumbling motion of the most localized waters of hydration with increasing strain. This observation appears to be correlated with the observation that the lifetime of hydrogen bonds formed between the model peptide $(VPGVG)_3$ and water decreases upon extension, as noted in Table 3. Given that the deformation is applied to the protein backbone, it appears that the changes to the dynamics of the localized waters of hydration are driven by an increase in the frequency of oscillation of the backbone. As further evidence of the correlated water–protein behavior, the residual quadrupolar interaction of localized water in elastin was recently measured in our laboratory by an NMR deuterium double quantum filter experiment.[39] As the temperature in this experiment was raised, we observed an increase in the residual quadrupolar interaction of water, which is a measure of the extent to which the quadrupolar interaction is partially averaged due to anisotropic motion, near the transition temperature of the protein.

From statistical mechanics it is well-known that reduction in entropy of a strained polymer results in the development of an entropic force, F_{Ent}, given by

$$F_{Ent} = -T\frac{\delta S}{\delta L} \quad (6)$$

where δS is the change in entropy of the system, δL is the change in length, and T is the temperature of the system.[40] The driving mechanism of elasticity is thus due to the reduction of the protein backbone entropy and the system is driven back to maximum entropy via the second law of thermodynamics when the applied force is removed. This behavior is analogous to the well-known statistical mechanical treatment of the classical theory of rubber elasticity–the entropy of the elastomer decreases with increasing strain.[41] The presence of a solvent is a required, albeit complex "lubricating" element for this highly cross-linked biological elastomer. The dependence of Young's modulus, for example, has been experimentally observed to depend on the viscosity of the solvent and its ability to penetrate into the intrafibrillar space.[42,43] As a hydrated biopolymer, the vibrational motion of elastin's backbone increases with increasing strain, analogous to a string on a musical instrument, resulting in a reduction in entropy and the development of an entropic elastomeric force.

CONCLUSIONS

In this work, we have implemented a deuterium 2D T_1–T_2 NMR correlation experiment to study the dynamical properties of the localized waters of hydration in mechanically strained elastin. As the applied strain is increased, the correlation time of the random tumbling motion of ^{2}H nuclei in water is observed to decrease, indicating an increase in the orientational entropy of localized water. A separate set of experiments were performed to measure the dynamics of the carbonyl and aliphatic carbons of the protein backbone as a function of applied strain. Our experimental findings indicate that the carbonyl and aliphatic carbon correlation times, corresponding to the overall ^{1}H–^{13}C dipolar interactions, decrease with increasing strain. Short 4 ns molecular dynamics simulations of a small toy-model elastin peptide, $(VPGVG)_3$, were used to demonstrate that the population of vibrational modes of the peptide shift to high frequency when the system is placed under strain. The increase in vibrational frequency of the model peptide under strain correlates well with the observed trends in the experimental measurements of the carbonyl and aliphatic carbon correlation times. It is argued that the shift in vibration modes reduces the protein backbone entropy resulting in the development of an entropic elastomeric force. The methods implemented in this study may prove to be useful in studies aimed at enhancing the elasticity of artificial elastomers[44,45] or in furthering the understanding of elastin degradation in various connective tissue disorders.[46,47]

Acknowledgments

The authors thank Yi-Qiao Song for use of the 2D ILT algorithm and Steven Morgan, Raymond Tung, Alexej Jerschow, Ranajeet Ghose, Nicolas Giovambattista, Laura Juszczak, and Richard Magliozzo for useful discussions. G.S.B. acknowledges support from NIH grant no. 7SC1GM086268-03. The content is solely the responsibility of the authors and does not necessarily represent the official views of the National Institute of General Medical Sciences or the National Institutes of Health.

REFERENCES

1. Urry DW. J. Protein Chem. 1988; 7:1–34. [PubMed: 3076447]
2. Debelle L, Tamburro AM. Int. J. Biochem. Cell Biol. 1999; 31:261–272. [PubMed: 10216959]
3. Muiznieks LD, Weiss AS, Keeley FW. Biochem. Cell Biol. 2010; 88:239–250. [PubMed: 20453927]
4. Lillie MA, Gosline JM. J. Biorheol. 1993; 30:229–242.
5. Partridge SM, Davies HF, Adair GS. Biochem. J. 1955; 61:11–20. [PubMed: 13260170]
6. Mistrali F, Volpin D, Garibaldo GB, Ciferri A. J. Phys. Chem. 1971; 76:142–150. [PubMed: 5167451]
7. Hoeve CAJ, Flory PJ. Biopolymers. 1974; 13:677–686. [PubMed: 4847581]

8. Weis-Fogh T, Anderson SO. Nature. 1970; 227:718–721. [PubMed: 5432073]
9. Gary WR, Sandberg LB, Foster JA. Nature. 1973; 246:21–28.
10. Mammi M, Gotte L, Pezzin G. Nature. 1968; 220:371–373. [PubMed: 5684878]
11. Li B, Alonso DOV, Daggett V. J. Mol. Biol. 2001; 305:581–592. [PubMed: 11152614]
12. Schreiner E, Nicolini C, Ludolph B, Ravindra R, Otte N, Kohlmeyer A, Rousseau R, Winter R, Marx D. Phys. Rev. Lett. 2004; 92 148101–1-4.
13. Urry DW, Parker TM. J. Muscle Res. Cell Motil. 2002; 23:543–559. [PubMed: 12785104]
14. Song Y-Q, Venkataramanan L, Hürlimann MD, Flaum M, Frulla P, Straley C. J. Magn. Reson. 2002; 154:261–268. [PubMed: 11846583]
15. Fung BM, Khitrin AK, Ermolaev K. J. Magn. Reson. 2000; 142:97–101. [PubMed: 10617439]
16. Duer, MJ. Introduction to Solid-State NMR Spectroscopy. Oxford, UK: Blackwell Publishing Ltd.; 2004.
17. Jorgensen WL, Tirado-Rives J. J. Am. Chem. Soc. 1988; 110:1657–1666.
18. Berendsen HJC, Postma JPM, DiNola A, Haak JR. J. Chem. Phys. 1984; 81:3684–3690.
19. Hess B, Kutnzer C, Spoel DVD, Lindahl E. J. Chem. Theory Comput. 2008; 4:435–477.
20. Teleman O, Jonsson B, Engstrom S. Mol. Phys. 1987; 60:193–203.
21. Zimmerman K. J. Comput. Chem. 1991; 12:310–319.
22. Hills B, Costa A, Marighet N, Wright K. Appl. Magn. Reson. 2005; 28:13–27.
23. McDonald PJ, Korb JP, Mitchell J, Monteilhet L. Phys. Rev. E. 2005; 72 011409-1–9.
24. Sun C, Boutis GS. New J. Phys. 2011; 13:025026–025042.
25. Abragam, A. Principles of Nuclear Magnentism. New York: Oxford University Press; 1961.
26. Li B, Alonso DOV, Bennion BJ, Daggett V. J. Am. Chem. Soc. 2001; 123:11991–11998. [PubMed: 11724607]
27. Perry A, Stypa MP, Tenn BK, Kumashiro KK. Biophys. J. 2002; 82:1086–1095. [PubMed: 11806948]
28. Yao XL, Conticello PL, Hong M. Magn. Reson. Chem. 2004; 42 267-27.
29. Peng JW, Thanabal V, Wagner G. J. Magn. Reson. 1991; 94:82–100.
30. Torchia DA, Piez KA. J. Mol. Biol. 1973; 76:419–424. [PubMed: 4738731]
31. Rauscher S, Baud S, Miao M, Keeley FW, Pomes R. Structure. 2006; 14:1667–1676. [PubMed: 17098192]
32. He D, Chung M, Chan E, Alleyne T, Ha KCH, Miao M, Stahl RJ, Keeley FW, Parkinson. J. Matrix Biol. 2007; 26:524–540.
33. Andricioaei I, Karplus M. J. Chem. Phys. 2001; 115:6289–6292.
34. Lei W, Tan HH, Jagadish C, Ren QJ, Lu J, Chen ZH. Appl. Phys. Lett. 2010; 97 223108-1-3.
35. Groenen J, Mlayah A, Carles R, Ponchet A, Le Corre A, Salaüun S. Appl. Phys. Lett. 1996; 67:943–945.
36. Siakavellas M, Kontos AG, Anastassakis E. J. Appl. Phys. 1998; 84:517–521.
37. Cronin SB, Swan AK, Unlu MS, Goldberg BB, Dresselhaus MS, Tinkham M. Phys. Rev. B. 2005; 72 035425-1–6.
38. Milekhin AG, Nikiforov AI, Yu M, Ladanov A, Pchelyakov OP, Schulze S, Zahn DRT. Mater. Res. Soc. Symp. Proc. 2003; 737:E13.7.1–E13.7.6.
39. Cheng S, Boutis GS. J. Magn. Reson. 2010; 205:86–92. [PubMed: 20452263]
40. Reif, F. Fundamentals of Statistical and Thermal Physics. New York: McGraw-Hill; 1965.
41. Flory, PJ. Statistical Mechanics of Chain Molecules. New York: Butterworth- Heinemann; 1969.
42. Winlove CP, Parker KH. Biopolymers. 2004; 29:729–735. [PubMed: 2383639]
43. Lillie MA, Gosline JM. Biopolymers. 1990; 5:1147–1160. [PubMed: 2369629]
44. Huang L, McMillan RA, Apkarian RP, Pourdeyhimi B, Conticello VP, Chaikof EL. Macromolecules. 2000; 33:2989–2997.
45. Pepe A, Armenante AM, Bochicchio B, Tamburro AM. Soft Matter. 2009; 5:104–113.

46. Abraham PA, Perejda AJ, Carnes WH, Uitto J. J. Clin. Invest. 1982; 70:1245–1252. [PubMed: 7174792]

47. Chowdhury T, Reardon W. Pediatr. Cardiol. 1999; 20:103–107. [PubMed: 9986885]

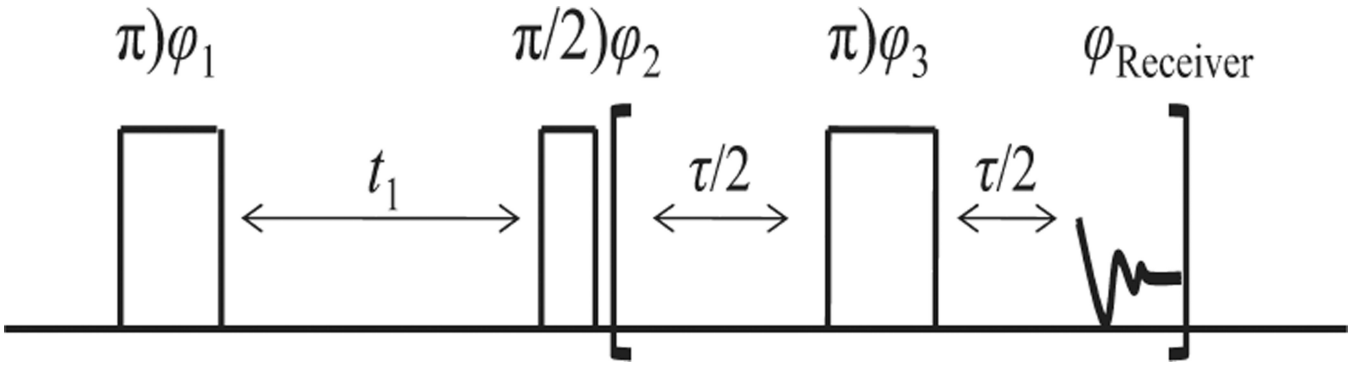

Figure 1.
NMR pulse sequence used for ^{2}H 2D T_1–T_2 correlation experiments in this work. In the experiments, $\varphi_1 = x, -x, \varphi_2 = x, x, -x, -x, \varphi_3 = y$ and $\varphi_{receiver} = x, x, -x, -x$. The experimental values for t_1 and τ are described in the text.

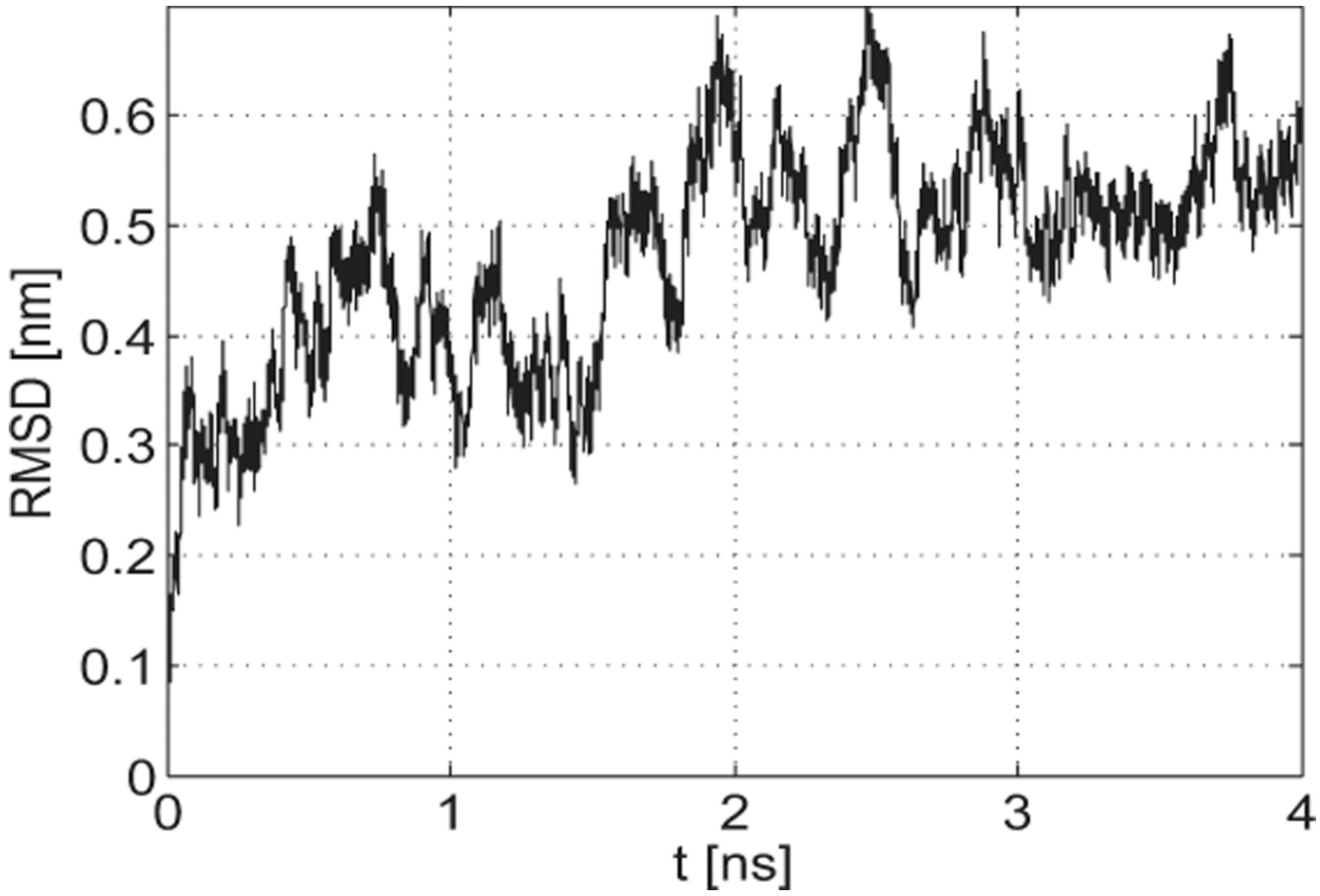

Figure 2.

Resulting root-mean-square displacement (rmsd) averaged over all C_α atoms as a function of time in the MD simulation of the 15-residue model elastin peptide $[VPGVG]_3$. In our analysis of the characteristics of the unstrained peptide, data from 3 to 4 ns was used. For the simulation where a force was applied, the structure after 2 ns was used as the starting structure, as described in Materials and Methods.

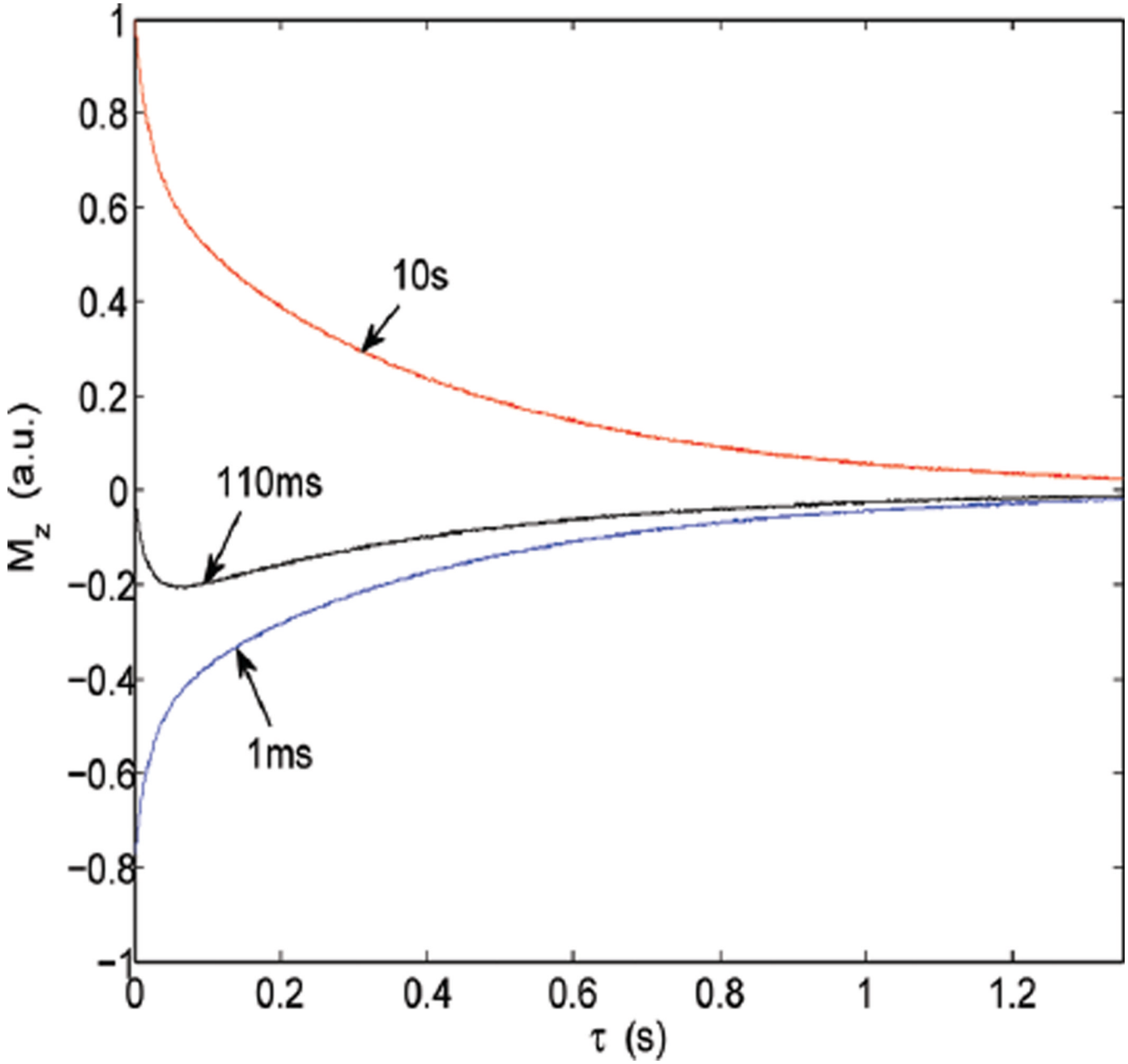

Figure 3.

Sample raw data resulting from the ^{2}H 2D T_1–T_2 correlation experiment using the pulse sequence shown in Figure 1, on sample I. The figure shows selected slices from the 2D map for t_1 = 1 ms, 110 ms, and 1s. By performing a 2D ILT of the experimental data, one obtains a correlation map that correlates T_1 to T_2 shown in Figure 4.

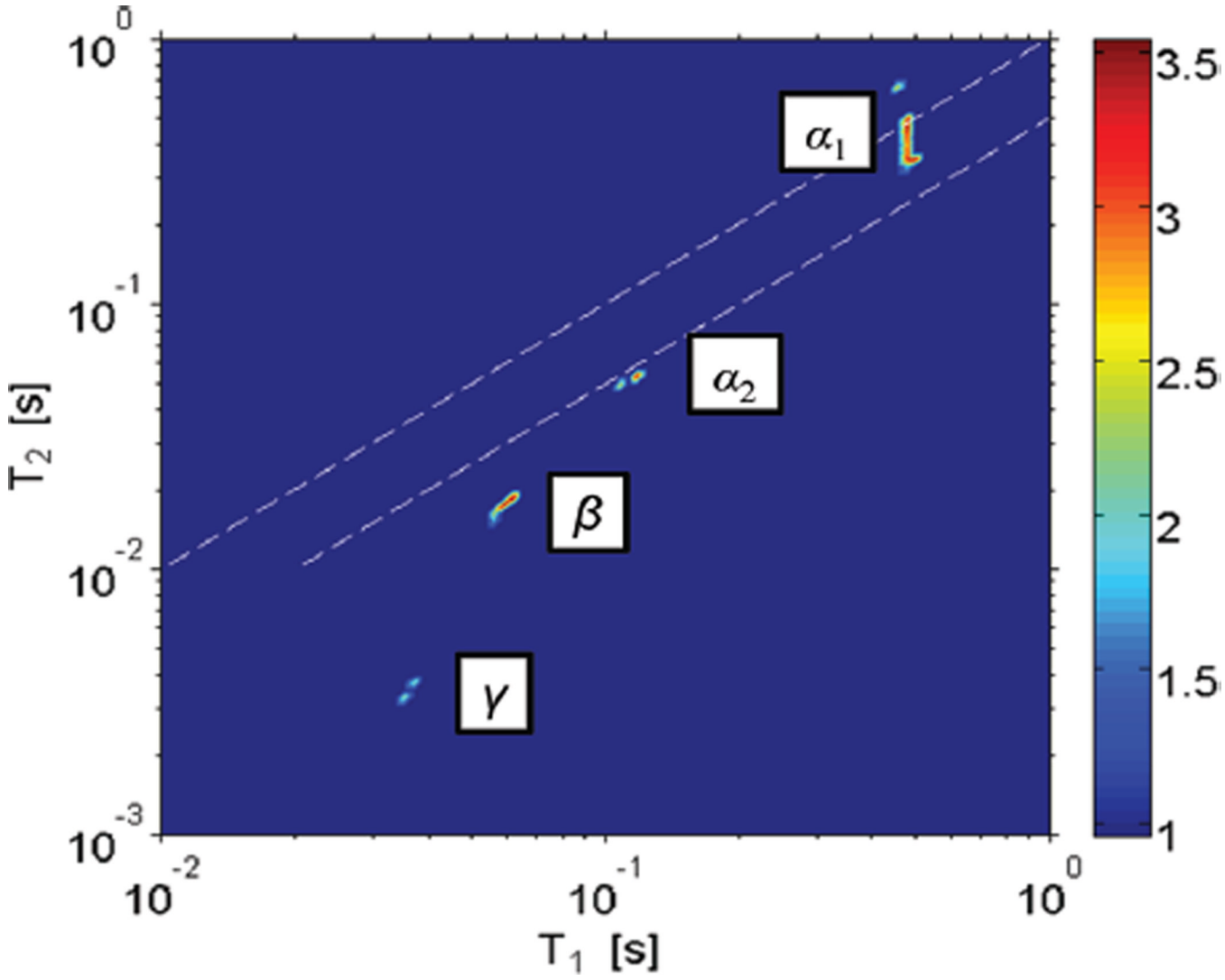

Figure 4.

^{2}H 2D ILT map of the T_1–T_2NMR relaxation times of water in sample I, defined in the text. Four components are discernible and are labeled α_1, α_2, β, and γ. The dashed lines are used to guide the eye for the region of the 2D map where T_1 is approximately equal to T_2. The signal intensity, indicated by the color bar, is shown on a logarithmic scale.

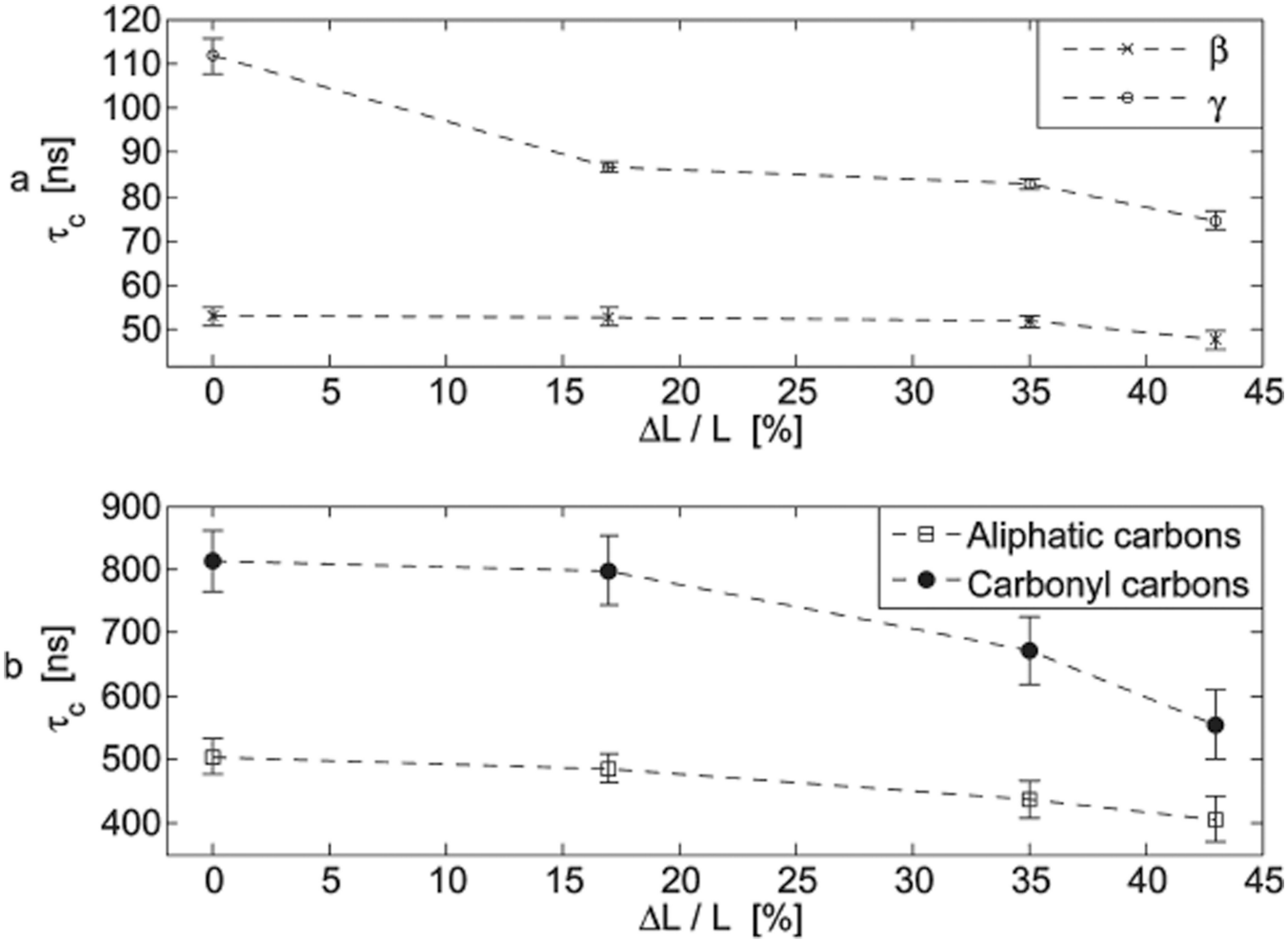

Figure 5.

Measured correlation times as a function of the applied strain. (a) Correlation times of the fluctuating quadrupolar field of D_2O in close proximity to elastin (open circles for component γ and crosses for component β), as determined from eqs 1 and 2 and the measured ^2H T_1 and T_2. (b) Correlation times characterizing the fluctuating dipolar field experienced by the carbonyl (closed circles) and aliphatic carbons (open squares) of elastin, as determined from eqs 3 and 4 and the measured ^{13}C T_1 and $T_{1\rho}$. The dashed lines are used to guide the eye. The error bars shown in the graphs represent the errors propagated from the errors in the measured relaxation times.

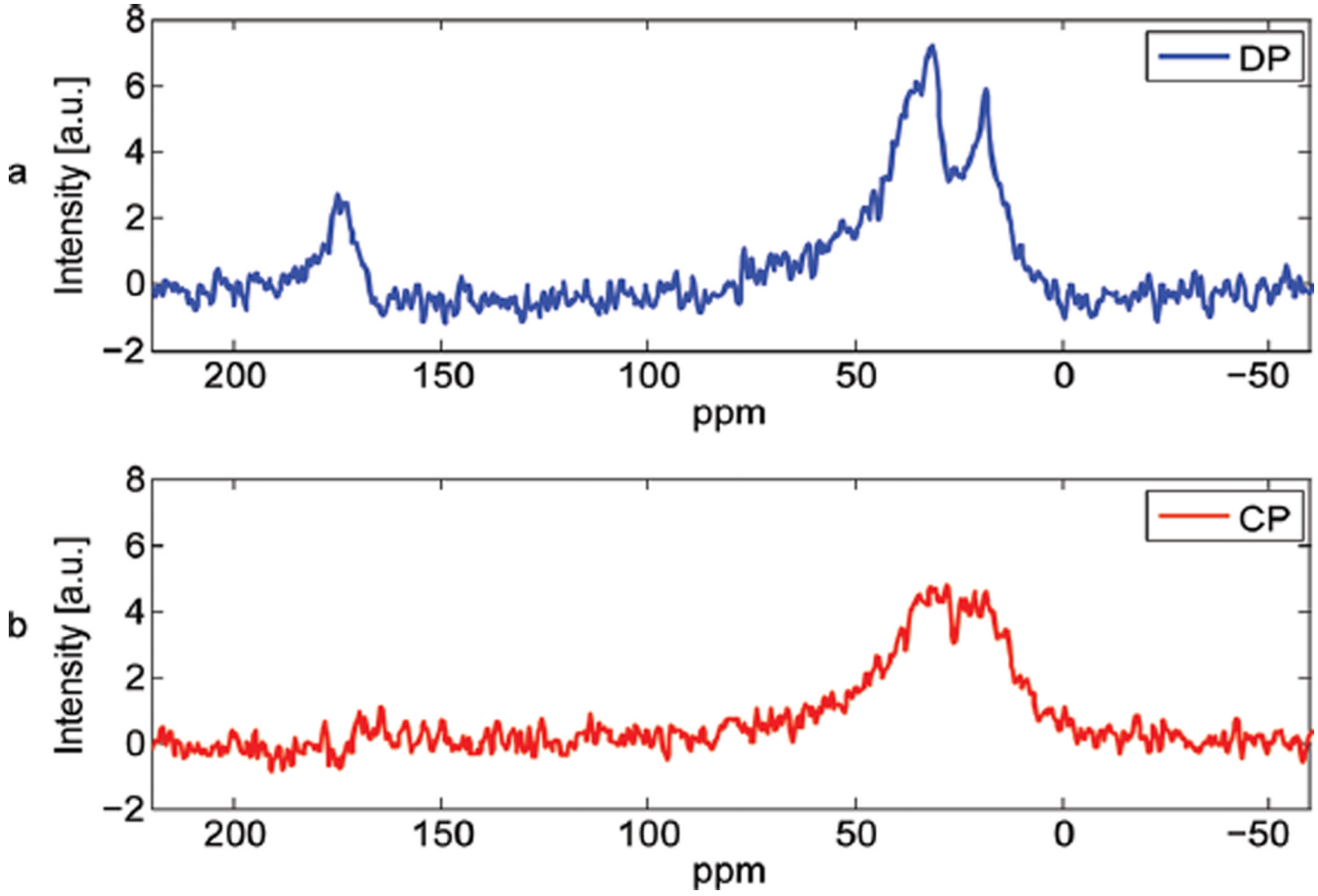

Figure 6.

Natural abundance ^{13}C NMR spectra of sample I, defined in the text. (a) Direct polarization (DP) and (b) $^{1}H \rightarrow {}^{13}C$ cross polarization (CP). The contact time for $^{1}H \rightarrow {}^{13}C$ CP was 1.4 ms. The data shown were accumulated with 14512 scans, with a recycle delay of 5s. All spectra are referenced to adamantane.

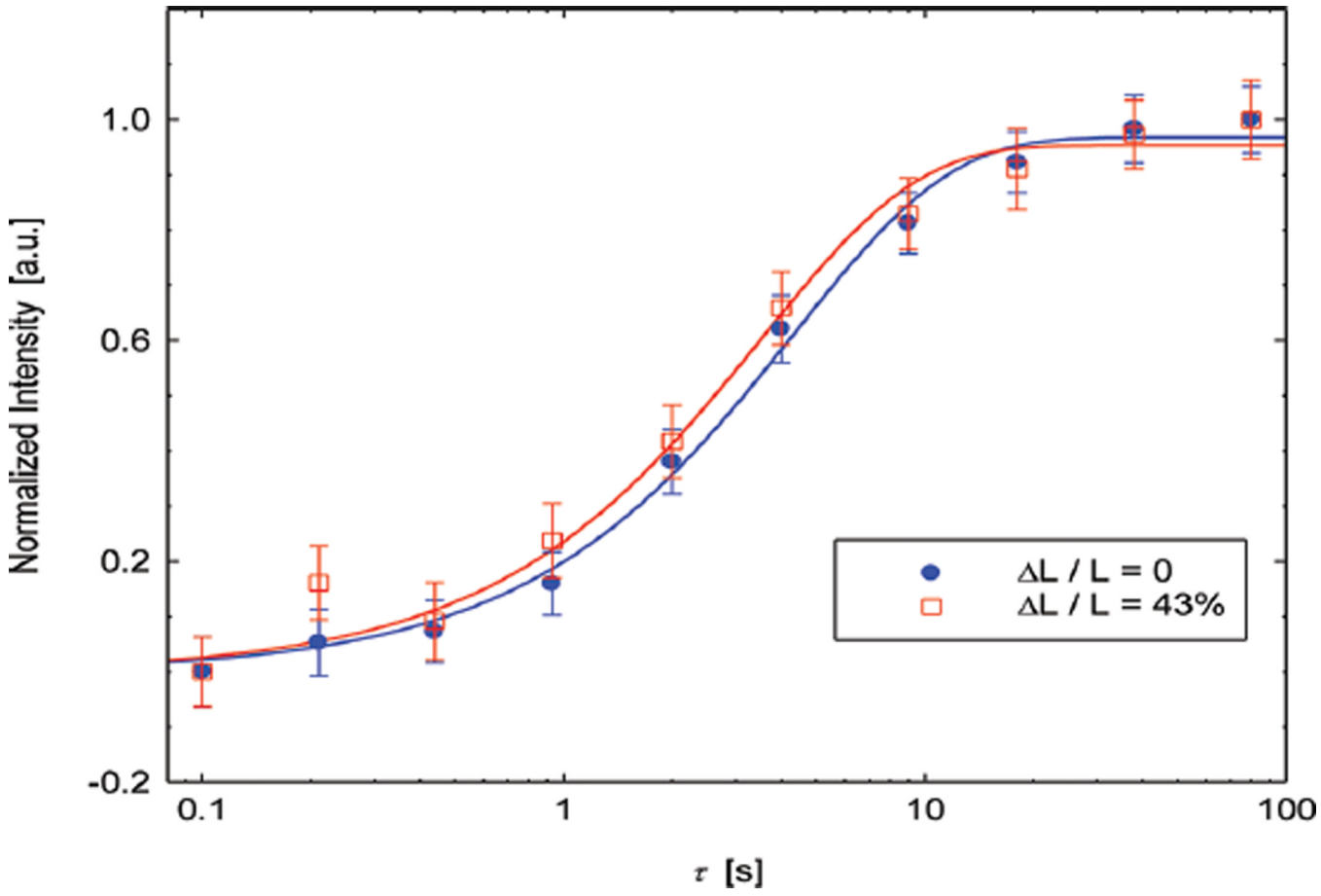

Figure 7.

Sample experimental results from the carbonyl ^{13}C T_1 measurements for the relaxed and 43% strained elastin. The solid lines shown in the figure are a best fit to a theoretical model for a saturation recovery experiment. For the relaxed sample data $\chi^2/\nu = 0.26$ and $\chi^2/\nu = 0.53$ for the 43% strained sample. The error bar shown in the graph represents the error in our measured signal intensity.

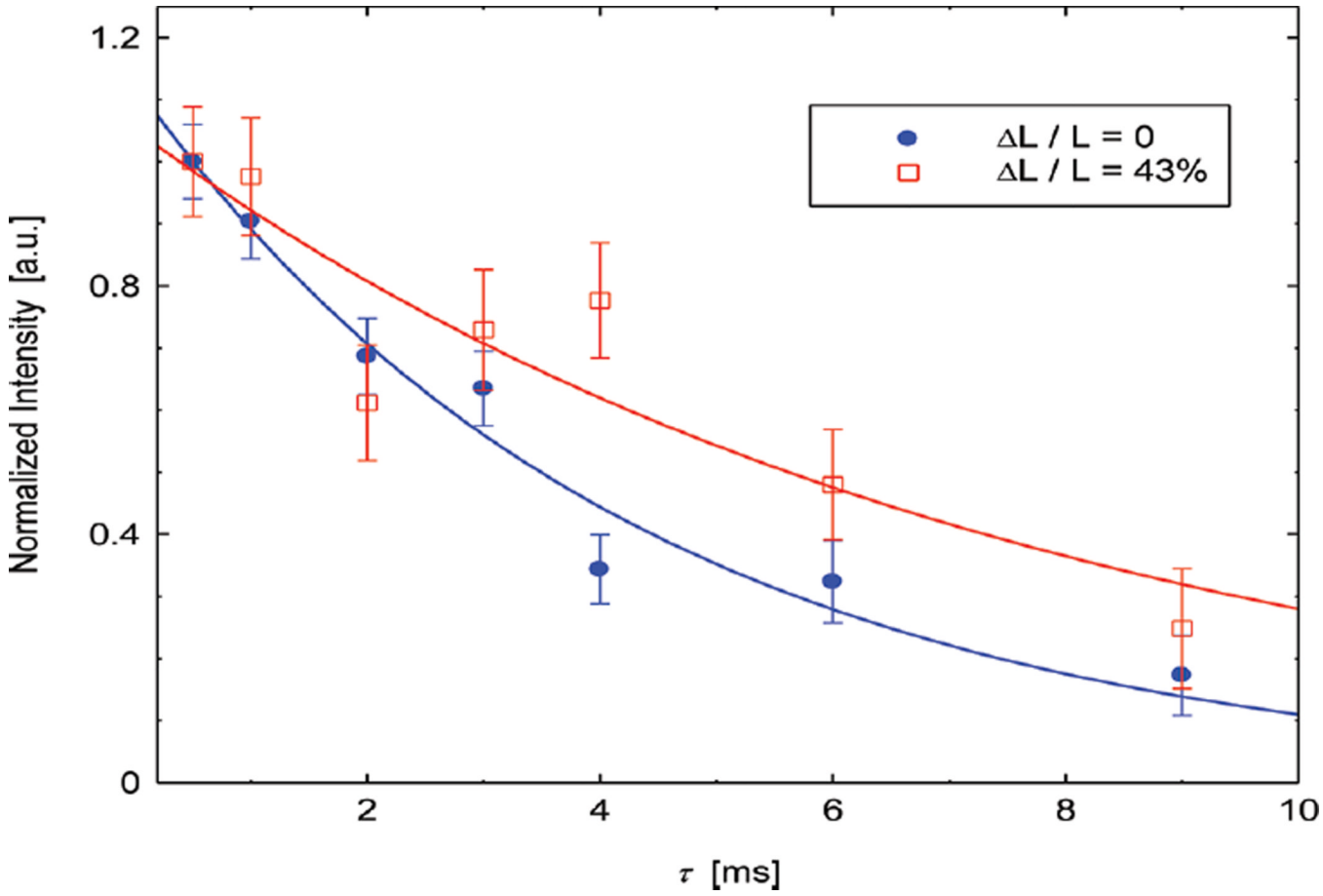

Figure 8.

Sample experimental results from the carbonyl ^{13}C $T_{1\rho}$ measurements for the relaxed and 43% strained elastin. The solid lines shown in the figure are a best fit to single exponential decay. For the relaxed sample data $\chi^2/\nu = 1.13$ and $\chi^2/\nu = 1.65$ for the 43% strained sample. The error bar shown in the graph represents the error in our measured signal intensity.

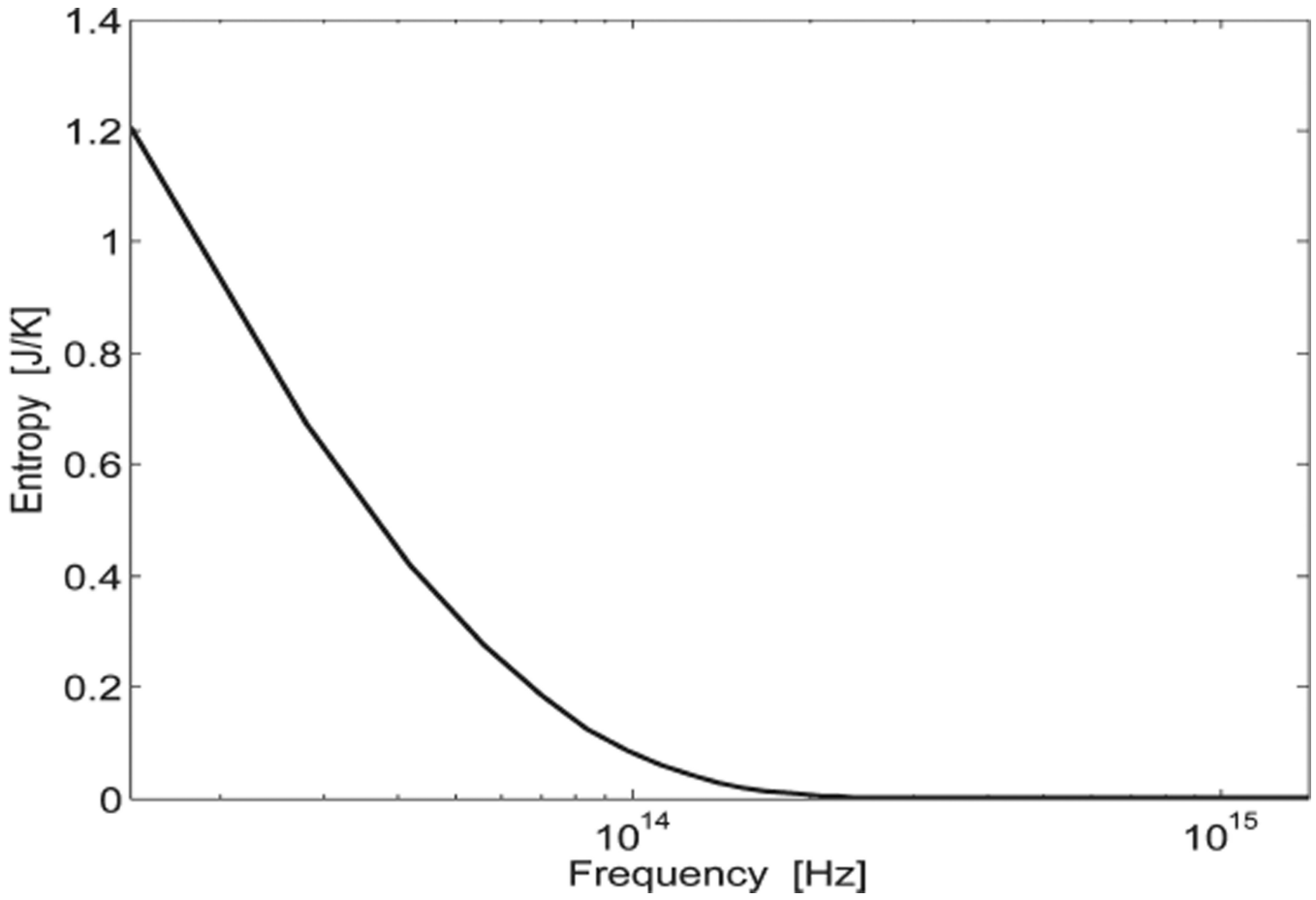

Figure 9.
Graph of the dependence of the entropy of a harmonic oscillator, based on eq 5, as a function of frequency.

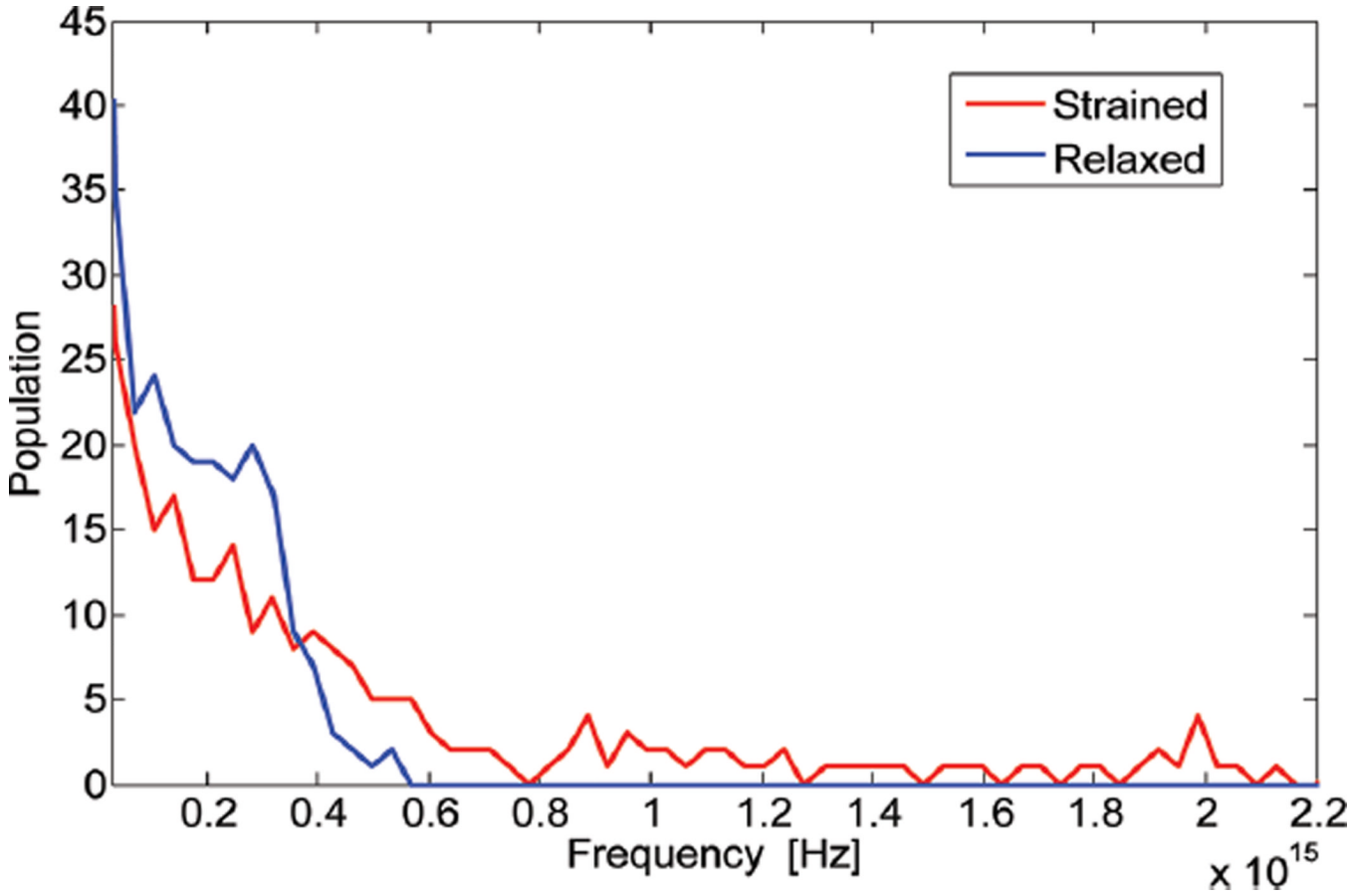

Figure 10.
Histogram of frequencies derived from the quasi-harmonic approach in the MD simulations of the elastin mimetic peptide $(VPGVG)_3$ under relaxed (blue line) and strained (red line) states.

Table 1

Experimental Results of ^{2}H NMR Relaxation Times T_1 and T_2 for the γ and β Water Components in Elastin, As Described in the Text[a]

samples	I	II	III	IV	V
			γ Component		
T_1(ms)	35.1± 1.0	40.4 ±1.9	30.5 ± 1.3	40.4 ± 1.9	40.4 ± 1.9
T_2 (ms)	3.3 ± 0.2	5.7 ± 0.4	4.6 ± 0.3	7.1 ± 0.5	3.8 ± 0.3
τ_c(s)	(1.12 ± 0.05) × 10^{-7}	(8.67 ± 0.13) × 10^{-8}	(8.29 ± 0.13) × 10^{-8}	(7.46 ± 0.13) × 10^{-8}	(1.12 ± 0.02) × 10^{-7}
C_q (s^{-2})	(2.11 ±0.04) × 10^{10}	(1.46 ± 0.08) × 10^{10}	(1.87 ±0.11) × 10^{10}	(1.29 ± 0.09) × 10^{10}	(1.83 ± 0.13) × 10^{10}
			β Component		
T_1 (ms)	55.9 ± 2.7	64.3 ± 2.9	50.9 ± 2.3	46.4 ± 2.1	67.3 ± 3.2
T_2 (ms)	15.2 ± 2.3	17.5 ± 1.2	14.2 ± 1.0	14.2 ± 1.0	18.7 ± 1.4
τ_c(s)	(5.31 ± 0.43) × 10–^{8}	(5.30 ± 0.22) × 10^{-8}	(5.19 ± 0.12) × 10^{-8}	(4.78 ± 0.20) × 10^{-8}	(5.21 ± 0.12) × 10^{-8}
C_q (s^{-2})	(7.28 ± 0.70) × 10^9	(6.33 ± 0.39) × 10^9	(7.88 ± 0.50) × 10^9	(8.20 ± 0.52) × 10^9	(5.97 ± 0.35) × 10^9

[a]In the table, τ_C and C_q (defined in the text) were determined by using eqs 1 and 2 and the ^{2}H T_1 and T_2 relaxation times. The respective values shown after the ± represent standard error from the measurements.

J Phys Chem B. Author manuscript; available in PMC 2013 April 11.

Table 2

Experimental Results of ^{13}C NMR Relaxation Times T_1 and $T_{1\rho}$ for Water Hydrated Elastin[a]

samples	I	II	III	IV	V
			Carbonyl Carbons		
T_1(s)	4.3 ±0.3	5.0 ± 0.4	4.1 ± 0.4	3.5 ± 0.4	4.2 ± 0.4
$T_{1\rho}$ (ms)	4.3 ± 0.2	5.2 ± 0.3	6.0 ± 0.4	7.5 ± 0.7	4.6 ± 0.3
τ_c(s)	(8.14 ± 0.48) × 10^{-7}	(7.98 ± 0.54) × 10^{-7}	(6.72 ± 0.54) × 10^{-7}	(5.55 ± 0.55) × 10^{-7}	(7.78 ± 0.64) × 10^{-7}
C_D (s^{-2})	(1.43 ± 0.02) × 10^8	(1.21 ± 0.01) × 10^8	(1.24 ± 0.02) × 10^8	(1.20 ± 0.02) × 10^8	(1.40 ± 0.02) × 10^8
			Aliphatic Carbons		
T_1(s)	0.90 ± 0.06	0.68 ± 0.05	0.98 ± 0.07	0.94 ± 0.07	0.93 ± 0.11
$T_{1\rho}$ (ms)	2.34 ± 0.14	1.90 ± 0.09	3.39 ± 0.25	3.78 ± 0.36	2.47 ± 0.29
τ_c(s)	(5.04 ± 0.28) × 10^{-7}	(4.86 ± 0.23) × 10^{-7}	(4.37 ± 0.30) × 10^{-7}	(4.05 ± 0.36) × 10^{-7}	(4.99 ± 0.55) × 10^{-7}
C_D (s^{-2})	(4.23 ± 0.02) × 10^8	(5.40 ± 0.06) × 10^8	(3.37 ± 0.02) × 10^8	(3.26 ± 0.03) × 10^8	(4.06 ± 0.03) × 10^8

[a]In the table, τ_C and C_D (defined in the text) were determined by using eqs 3 and 4 and the ^{13}C T_1 and $T_{1\rho}$ relaxation times. The respective values shown after the ± represent standard error from the measurements.

Table 3

Molecular Dynamics (MD) Simulation Results for an Elastin Mimetic Peptide $(VPGVG)_3$ under Relaxed and Strained States[a]

	relaxed	strained
peptide entropy (kJ/(mol K))	1.63	1.46
no. of H_2O within 0.6 nm of peptide	1132 ± 248	5451 ± 177
average rmsf of C^{α}(nm)	0.19 ± 0.05	0.14 ± 0.06
radius of gyration of C^{α}(nm)	0.78 ± 0.07	0.83 ± 0.03
lifetime of peptide–water H-bond (ps)	0.87 ± 0.05	0.53 ± 0.02

[a]In the table, peptide–water H- bonds were counted when the donor–acceptor cutoff distance of 0.35 nm and the hydrogen–donor–acceptor angle of 30° were satisfied. The respective values shown after the ± are standard deviations determined by the fluctuations in the MD simulation.